ELSEVIER

Journal of Fluids and Structures 24 (2008) 1227–1239

JOURNAL OF FLUIDS AND STRUCTURES

www.elsevier.com/locate/jfs

The effect of end conditions on the vortex-induced vibration of cylinders

T.L. Morse[a], R.N. Govardhan[b], C.H.K. Williamson[a,*]

[a]*Sibley School of Mechanical and Aerospace Engineering, Upson Hall, Cornell University, Ithaca, NY 14853, USA*
[b]*Department of Mechanical Engineering, Indian Institute of Science, Bangalore 560012, India*

Received 25 March 2008; accepted 8 June 2008
Available online 23 October 2008

Abstract

In the present investigation we study the effect of end conditions on the vortex-induced vibration of an elastically mounted rigid cylinder. This work was triggered by some initial controlled vibration experiments which showed that spanwise end conditions can have a large effect on measured fluid forces on a cylinder, and this suggested that some of the disparity amongst previous free vibration studies may possibly be attributed to differences in end conditions. In the principal experiments here, we are concerned with a vertical cylinder piercing the clean free surface of a water channel, and attached to a carriage system mounted atop the channel. The upper end of the submerged cylinder is thus the free surface, while the lower end is manipulated to yield three different conditions, namely: an attached endplate; an unattached endplate fixed to the channel floor (with a variable gap between cylinder and plate); and a condition of no endplate at all. Interestingly, we find that the free vibration response for the attached and unattached endplate cases were nearly identical. One expectation was that the case *without* an endplate would lead to a flow around the end of the body, modifying the vortex dynamics, and thereby reducing the correlation of the induced fluid forces on the body. Surprisingly, over the entire response plot, *the vibration amplitude is markedly higher in the absence of an endplate*, with the exception of the peak amplitude, which remains nearly unchanged. Unexpectedly, the vibrations become much more steady at flow velocities in the vicinity of the peak response, if the endplate is removed. In a further set of experiments, we undertake controlled vibration, where we vary the gap between cylinder and endplate. We discover a large discontinuous jump in the magnitude of fluid excitation, when the gap exceeds 15% of a diameter. For larger gaps, the fluid excitation becomes independent of the gap size, effectively equivalent to having no plate at all. This study is consistent with some of the disparity between the character of vibration response plots in previous studies, if one takes into account the particular end conditions chosen in those studies.

Keywords: Vortex-induced vibration; End conditions; Circular cylinder

1. Introduction

Vortex-induced vibration is an important problem in many fields of engineering. It affects the dynamics of riser tubes bringing oil from the seabed to the surface, as well as civil engineering structures such as bridges, chimneys, and

*Corresponding author. Tel.: +1 607 255 9115; fax: +1 607 255 1222.
E-mail address: cw26@cornell.edu (C.H.K. Williamson).

0889-9746/$ - see front matter
doi:10.1016/j.jfluidstructs.2008.06.004

buildings, and is cause for concern in many other practical applications. The range of problems caused by vortex-induced vibration has led to a large number of experimental and computational studies on the subject, including several review articles, for example: Sarpkaya (1979), Griffin and Ramberg (1982), Bearman (1984), Parkinson (1989), and more recently Williamson and Govardhan (2004).

In studies of vortex-induced vibration, the case of an elastically mounted rigid cylinder, constrained to move transverse to an incoming flow, is often used as a paradigm for understanding more diverse experimental arrangements. The present study of the effects of spanwise end conditions on free vibration response has actually been triggered by some recent experiments (Morse and Williamson, 2006), where we set out to conduct controlled vibrations of a body, and to make accurate comparisons with free vibration studies, involving measurements of fluid force, and predictions of amplitude. Our own free-vibration arrangement comprises a vertical cylinder, attached below an air-bearing carriage system sitting atop a water channel. The lower end of the submerged portion of the cylinder vibrates transversely above an endplate that is fixed to the channel floor. (It is noted briefly that we were careful to ensure "clean" free surface conditions, removing any dust film that may be present, and enabling the vortex lines to pass through the surface consistent with vortex formation parallel to the body.) At the outset, we were discouraged to find significant disparity between forces measured from our controlled experiments versus those measured for free vibration, under the same conditions of amplitude and frequency (see Fig. 1). It soon became apparent that the key to the large differences in fluid forces was due to the sensitivity of the flow around the body to small differences in the gap dimension between cylinder and endplate. Such effects are clearly seen in the force fluctuations exhibited in Fig. 1, showing marked differences for different gap sizes (different values of $g^* = \text{gap}/\text{diameter}$). On the other hand, if one ensures *precisely* the same experimental arrangements between the free and controlled vibration cases, one not only observes the fluid forces to be nearly identical, but one also finds highly accurate response prediction (as shown in Morse and Williamson, 2008). On the basis of these preliminary results, we can therefore expect differences in experimental end condition arrangements between different researchers to affect the free vibration response, as well as the fluid forcing from vortex dynamics.

A further interesting fact will emerge from the comparison of force fluctuations in Fig. 1. Upon inspection of these fluctuations, one would suspect that the more organized periodic forces for the small gap ($g^* = 0.05$) would provide a larger energy transfer from fluid to body motion, than would be found at the larger gap ($g^* = 0.44$), where the forces are less periodic. (One would naturally expect the vortex formation to be disrupted due to the flow around the ends.) In fact, the converse is true! The larger gap in (c) yields greater energy transfer, and the system would, if elastically mounted, increase its displacement amplitude; in essence, the larger gap would yield a larger vibration amplitude. This

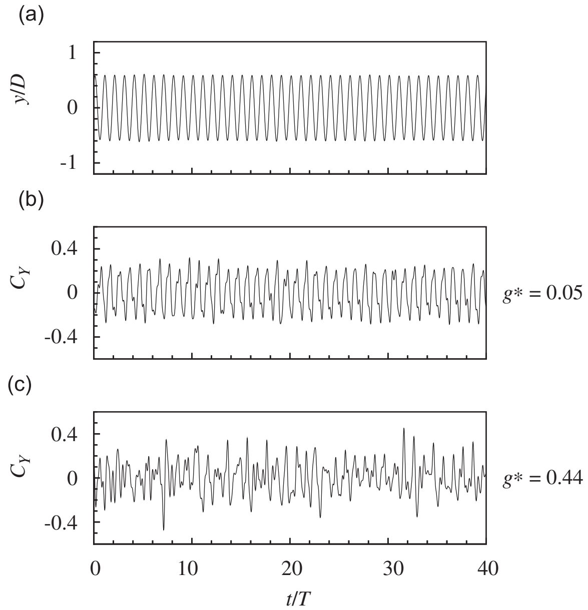

Fig. 1. Effects of the gap size (g^*) on the transverse force measurements (C_Y). In (a) we show the transverse displacement, y/D ($A^* = 0.60$, $U^*/f^* = 7.55$). Despite the fact that we matched closely the transverse displacement, the forces for low gaps in (b), $g^* = 0.05$ (free vibration) differ substantially from the forces for large gaps in (c), $g^* = 0.44$ (controlled vibration). We deduce that these differences are due to the sensitivity of the flow to gap size, $g^* = \text{gap}/\text{diameter}$.

counter-intuitive result has been part of the stimulus for this paper. One of the keys to understanding this result is the fact that increasing the gap also modifies the phase between fluid force and body motion (ϕ) such that the energy of excitation increases.

We are concerned, in this paper, primarily with low values of mass and damping for a vibrating structure, and therefore focus on experiments conducted in water facilities; namely, water channels and towing tanks. We mention here some of the variety of end conditions employed in previous experiments in water facilities. Research groups in Norway have primarily used towing tanks, with horizontal cylinders supported by struts from an elastic structure above the tank, with circular endplates attached to the cylinder ends (Anand and Tørum, 1985; Moe and Overvik, 1982; Vikestad et al., 2000). The group at MIT [for example, Hover et al. (1998)] have also been using a horizontal cylinder with attached endplates in their towing tank experiments. In their case, they have developed an ingenious technique involving representation of the mass, damping and stiffness on a computer, while the fluid force is actually measured from their cylinder in the tank. This *Virtual Cable Testing Apparatus* allows them to run "virtual" free vibration experiments. In the experiments of Sarpkaya (1995), he has also used a horizontal cylinder suspended by struts, but in his case the endplates were fixed to the tunnel walls with a small gap separating them from the cylinder.

Vertical cylinders have also been used, beginning with recent studies by Khalak and Williamson (1996), who used a vertical cylinder (in a water channel) that was suspended from a carriage mounted on air bearings. They used an unattached endplate fixed to the channel floor. Jauvtis and Williamson (2004) set up a pendulum for two degree-of-freedom experiments, with a cylinder suspended beneath it in a water channel, again using an unattached endplate, whereas Owen et al. (2001) for their pendulum arrangement, employed endplates fixed to the cylinder. Brankovic and Bearman (2006) have also conducted vertical cylinder experiments, but without endplates at all, leaving a small gap between the body and the channel floor (and allowing the possibility for the channel boundary layer to influence the end conditions). Klamo et al. (2006) also used a free end without endplates. In summary, these experimental arrangements indicate the variety of approaches to treating the end conditions, and *it must be expected that there will also be a variety of responses*, *due to the different end conditions*, *even if all other flow parameters are kept constant*. The expectation of such differences is part of the stimulus of this study.

Much attention has been paid to the effect on free vibration response of varying experimental parameters such as mass and damping, and more recently, Reynolds numbers [see Govardhan and Williamson (2005, 2006), Klamo et al. (2005)]. Reynolds number is defined by $\mathrm{Re} = UD/\nu$, where U is the free stream velocity, D is the diameter, and ν is the kinematic viscosity. However, the effects of end conditions on free vibration response have been largely overlooked, and there has been no systematic study in the literature concerning the effects on response coming from different types of spanwise end configurations.

In the case of fixed cylinders in a flow, the end boundary conditions can have an important effect on the flow over both short cylinders (Slaouti and Gerrard, 1981), and over long cylinders even hundreds of diameters in length (Williamson, 1988, 1989, 1996). The vortex dynamics in the laminar regime ($\mathrm{Re} < 190$), and for moderate $\mathrm{Re} \sim 5000$ (Prasad and Williamson, 1997), are affected by end conditions. It is also well known that the length–diameter ratio (Szepessy and Bearman, 1992), and the end conditions, can affect the pressure distribution along the span (Stansby, 1974). One might suspect that body oscillations would reduce such effects, because vibration increases correlation lengths and vortex formation coherence along the span. However, Hover et al. (2004) have measured the correlation between fluid forces measured at both ends of a cylinder undergoing vortex-induced motion, and found that it drops significantly for oscillation frequencies below the natural vortex shedding frequency. Our present results will also show that a variation of end conditions has the most effect on response when the oscillation frequency is below the natural shedding frequency (in which case the normalized velocity exceeds the value corresponding to the peak amplitude response).

In the present work, we will principally be concerned with the effects of three different end boundary conditions, as illustrated in Fig. 2: the case of an unattached endplate (where we may vary the gap between cylinder and plate); an attached endplate; and the case of no endplate. As these boundary conditions are modified, we keep all other parameters, such as the cylinder dimensions, mass, damping and Reynolds number the same. We will also be primarily interested in experiments at high amplitude, under conditions of low mass and damping. In this case, previous studies have shown the existence of three branches of response (Khalak and Williamson, 1999), as illustrated in Fig. 3 (the solid symbols), namely the Initial branch (marked by the letter I), the Upper branch (U), and the Lower branch (L). There are therefore two mode transitions in this case. The first transition between the initial–upper branch is hysteretic, while the second one between the upper–lower branch involves an intermittent switching of modes. The transitions and their relationship with vortex dynamics modes and fluid forces were studied in detail by Govardhan and Williamson (2000). With respect to the present study, we wish to know how the end boundary conditions might affect the character of these response branches, their peak amplitudes, their regime of synchronization, and the possible changes to the mode transitions.

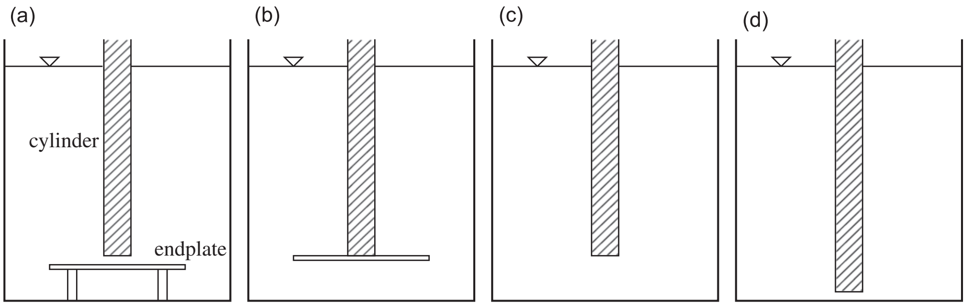

Fig. 2. Schematic diagram of some typical end conditions: (a) unattached endplate, with a small gap between the endplate and the bottom of the cylinder, (b) attached endplate, (c) free end, (d) cylinder end close to the channel floor.

We shall describe the experimental approaches in Section 2. The influence of end conditions on free vibration response are studied in Section 3, while the effects of end conditions on forces measured in controlled vibration are included in Section 4. Brief comparisons with previous investigations, where various different end conditions are employed, are presented in Section 5, followed by the conclusions in Section 6.

2. Experimental details

Our free vibration experiments are conducted using a hydroelastic facility described in detail in Khalak and Williamson (1996). The cylinder is suspended vertically from a carriage above the test section of the Cornell-ONR Water Channel. The carriage is attached to shafts which ride through air bearings. This system constrains the cylinder to move only transverse to the free stream flow, while ensuring very low structural damping. Springs of varying stiffness can be attached to the carriage to adjust the system elasticity, and mass can be added to the carriage to vary the system mass ratio. The test section of the water channel has a cross section of 38.1 cm × 50.8 cm. The flow speed is varied in the range 10–32 cm/s, and the turbulence level in the test section is measured to be less than 0.9%. The cylinder diameter is 5.08 cm, and has a submerged depth of 40.6 cm, giving an aspect ratio (L/D) of 8, and a Reynolds number regime, $\mathrm{Re} = 5000-16\,000$ over a range of flow speeds. The transverse displacement is measured using a non-contact (magnetostrictive) position transducer. The reported amplitude is the average of the top 10% of the individual amplitude peaks, evaluated in the manner described by Hover et al. (1998). In our case, we measure this amplitude over a complete displacement time trace of several hundred cycles.

For our controlled vibration measurements, we use precisely the same cylinder, but in this case it is suspended from a transverse lead screw system, driven by a computer-controlled motor. A two-axis force balance, utilizing linear variable displacement transducers (LVDTs), was used to measure the lift and drag forces on the body. The inertial forces due to the oscillating structural mass are subtracted from the total measured force, to yield the fluid forces on the cylinder. Instantaneous phase measurements are obtained through use of the Hilbert transform [see Khalak and Williamson (1999)].

Our three end condition arrangements were exhibited earlier in Fig. 2. For the unattached endplate case, we can vary the gap, such that $g^* = 0.02-0.5$, where the smallest gap corresponds to close to 1 mm. The endplate is rectangular (50.8 cm × 36.8 cm wide) with rounded corners. The attached endplate is circular with a diameter of 20.3 cm (four times the cylinder diameter). In the case without an endplate, the bottom of the cylinder is about 7 cm from the channel floor.

In this paper, we will need to define the energy transfer between fluid and body motion, and present the relevant non-dimensional groups. We introduce here an equation of motion often used to represent the vortex-induced vibration of a cylinder in the transverse y-direction (perpendicular to the free stream) as follows:

$$m\ddot{y} + c\dot{y} + ky = F(t), \tag{1}$$

where m is the system mass, c the structural damping, k the spring stiffness, and $F(t)$ the fluid force in the transverse direction. When the body motion is synchronized with the vortex shedding, reasonable approximations to the force and motion are often given as

$$y = A\sin(\omega t), \tag{2}$$

$$F(t) = F_0 \sin(\omega t + \phi), \tag{3}$$

Table 1
Non-dimensional groups

Mass ratio	m^*	$\frac{m}{\pi\rho D^2 L/4}$
Damping ratio	ζ	$\frac{c}{2\sqrt{k(m+m_A)}}$
Velocity ratio	U^*	$\frac{U}{f_N D}$
Amplitude ratio	A^*	$\frac{A}{D}$
Frequency ratio	f^*	$\frac{f}{f_N}$
Transverse force coefficient	C_Y	$\frac{F}{(1/2)\rho U^2 DL}$
Gap ratio	g^*	$\frac{g}{D}$
Reynolds number	Re	$\frac{UD}{\nu}$

In the above groups, U is the free-stream velocity, f is the oscillation frequency, f_N is the natural frequency in water, D is the cylinder diameter, L is the submerged length, ρ is the fluid density, ν is the fluid kinematic viscosity, and g is the gap between the endplate and the cylinder. The added mass, m_A is given by $m_A = C_A m_d$, where m_d is the displaced fluid mass and C_A is the potential added mass coefficient ($C_A = 1.0$ for a circular cylinder).

where $\omega = 2\pi f$, f is the oscillation frequency. The phase angle (ϕ), between fluid force and body displacement, is crucial in determining the energy transfer from fluid to body motion, and hence in influencing the amplitude of oscillation. We select a set of relevant non-dimensional parameters in this problem, which are presented in Table 1.

The response amplitude and frequency may be derived in a straightforward manner, along the lines of Khalak and Williamson (1999), as follows:

$$A^* = \frac{1}{4\pi^3}\frac{C_Y \sin\phi}{(m^* + C_A)\zeta}\left(\frac{U^*}{f^*}\right)^2 f^*, \quad f^* = \sqrt{\frac{m^* + C_A}{m^* + C_{EA}}}, \tag{4,5}$$

where C_A is the potential flow added mass coefficient ($C_A = 1.0$ for a circular cylinder), and C_{EA} is an "effective" added mass coefficient that includes an apparent effect due to the total transverse force in phase with body acceleration ($C_Y \cos\phi$):

$$C_{EA} = \frac{1}{2\pi^3}\frac{C_Y \cos\phi}{A^*}\left(\frac{U^*}{f^*}\right)^2, \tag{6}$$

where these non-dimensional groups $\{A^*, U^*, f^*, C_Y, m^*\}$ are defined in Table 1.

The amplitude equation above (4) shows the importance of the normalized fluid excitation ($C_Y \sin\phi$) in determining the amplitude of vibration. For a system in steady state, the fluid excitation is balanced by the energy lost due to structural damping. Thus $C_Y \sin\phi$ will always be positive, and quite small for a system of low mass-damping. In controlled vibration experiments, the fluid excitation is often measured for a cylinder moving with a prescribed amplitude and frequency, and the above equations are used to make predictions about the free vibration response from these measurements.

3. Effect of end conditions on free vibration response

In this work we focus on systems with low mass–damping, with a mass ratio of $m^* = 9.3$, and a mass–damping of $(m^* + C_A)\zeta = 0.014$. We measure the free vibration response of the system, for varying end conditions, keeping all other aspects of the experimental arrangement the same.

3.1. Comparison between unattached endplate and no endplate

We are interested here in the classic case where there is an unattached endplate (with $g^* = 0.04$), and we shall compare this condition with having no endplate at all. Employing the endplate, our response shows the typical three

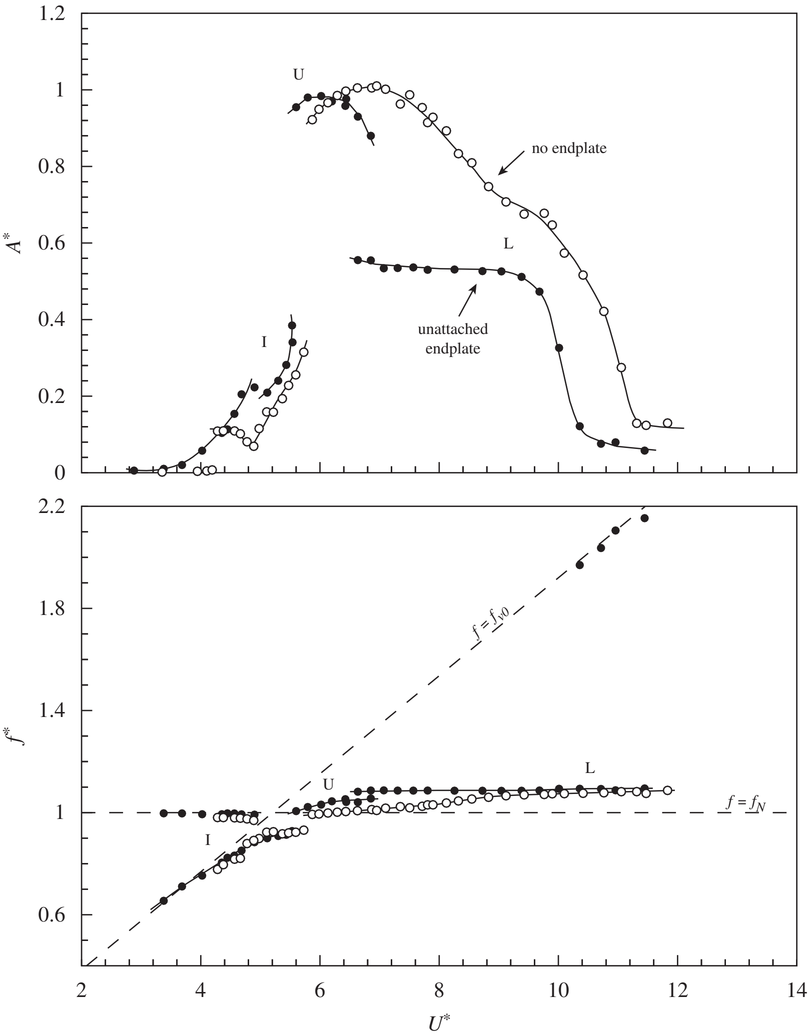

Fig. 3. Response amplitude (A^*) and frequency (f^*) as a function of the normalized fluid velocity (U^*). Comparison between the unattached endplate case, ($g^* = 0.04$) (•), and the case without an endplate (○). By removing the endplate, the amplitude diminishes continuously from its peak value, without evidence of a distinct upper and lower branch. $m^* = 9.3$, $(m^* + C_A)\zeta = 0.014$, $\mathrm{Re} = 5000-16\,000$.

branches: initial, upper, and lower (denoted with I, U, and L in Fig. 3). Without an endplate, two points can be made immediately from Fig. 3. Firstly, the amplitude decreases continuously, without clear evidence of an upper and lower branch. A consistent trend is found for the frequency response, in that the frequency, f^* increases gradually, without the characteristic jump in frequency associated with upper and lower response branches. Secondly, despite these distinct changes in the shape of the amplitude and frequency response, the peak amplitude remains almost precisely the same.

One might note that there is a horizontal shift between the response plots in Fig. 3, suggesting that some renormalization in the horizontal axis might be considered. A useful normalized velocity is given as $(U^*/f^*)S$, where $S = f_{VO}D/U$ is the Strouhal number for the non-oscillating body. This is equivalent to the parameter which relates the two most basic frequencies in the problem: f_{VO}/f, where f_{VO} is the vortex shedding frequency for the non-oscillating body and f the body oscillation frequency. Because of slight differences in the Strouhal number in the two sets of experiments [see also, Khalak and Williamson (1996)], the renormalized plot appears to line up reasonably in Fig. 4, in that the peak amplitudes, and the drop off in response at high U^*, occur at quite similar velocities. However, there is one major deduction to be made from this plot: over the entire plot, the amplitude level for the case without an endplate is higher, except right at the peak amplitude, where response is essentially the same. Without an endplate, one would

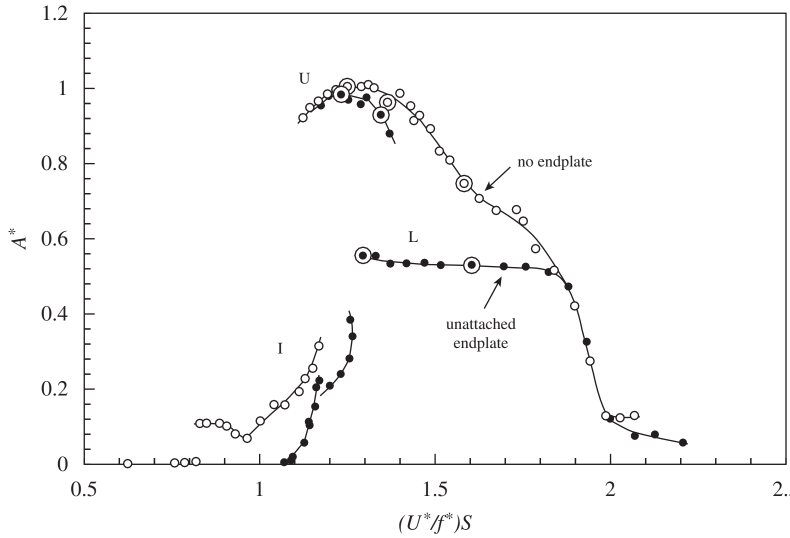

Fig. 4. Response amplitude (A^*) as a function of the normalized fluid velocity ($(U^*/f^*)S$). Comparison between the unattached endplate case, ($g^* = 0.04$) (●), and the case without an endplate (○). The bull's eyes indicate locations of displacement time traces shown in Fig. 5.

expect the vortex shedding to be disrupted by the flow around the end of the span, and for the shedding to be less correlated along the span, with smaller lift forces, and reduced response. One might therefore interpret the higher response in Fig. 4, when the endplate is removed, as counter-intuitive.

Concerning the upper–lower branch transition, we characterize the response now by observing briefly some typical time traces of body displacement, in Fig. 5. For the unattached endplate, in the upper branch, the cylinder response shows some significant variation in amplitude, as has typically been found in previous studies [for example, Khalak and Williamson (1996)]. At higher normalized velocity $(U^*/f^*)S = 1.35$, in the regime of upper-to-lower branch transition, the cylinder response shows an intermittent switching between a higher, but somewhat unsteady amplitude of the upper branch, and a lower but more steady amplitude of the lower branch. At still higher normalized velocity $(U^*/f^*)S = 1.60$, in the lower branch, the response becomes quite periodic.

However, by removing the endplate, we were surprised to find that the unsteady amplitude envelope, normally associated with the upper branch, is replaced by a remarkably steady vibration amplitude, shown clearly as $(U^*/f^*)S$ is increased through 1.25–1.58. Not only is the amplitude level increased generally, without the endplate, as we saw earlier, but the vibrations become much more steady if the endplate is removed, and the fluid is allowed to flow around the end.

3.2. Comparison between unattached endplate and attached endplate

In this section we investigate the case where the endplate is attached to the end of the cylinder, since it is a configuration commonly used in previous research studies. Our expectation in this case was that there would be distinct differences compared with the case of the unattached endplate. However, there is a strong similarity in both amplitude and frequency response, as shown in Fig. 6. Furthermore, although not shown here, the time traces of cylinder motion for the two cases were virtually indistinguishable. To emphasize this agreement, it is worth mentioning that the two data sets shown in Fig. 6 were taken eight years apart; the unattached endplate response was from a set of data taken in 1998 (along with the data that was eventually published in Govardhan and Williamson, 2000), while the attached endplate response was taken in 2006.

Our initial suspicion was that the extra fluid forces on the attached endplate, moving through the fluid with the cylinder, would have some effect to reduce the system response, by adding some "effective" damping. However, we deduce from the results here that any small forces on the endplate must be insignificant compared to the forcing due to the vortex shedding, and secondly that the vortex formation is effectively the same in the presence of an endplate, whether it is moving with the body or fixed with respect to the laboratory. Finally, on a practical note, we prefer to use the unattached endplate, because changing the test body will not entail each time the addition of a custom endplate, whose surface must be scrutinized to be parallel to the fluid flow.

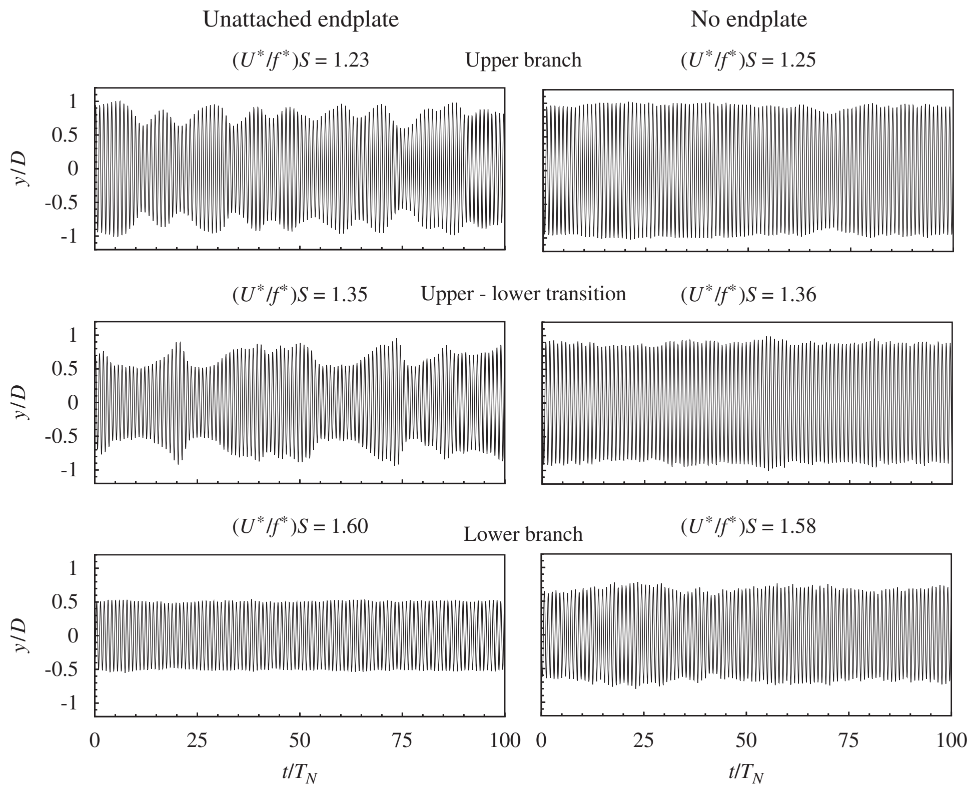

Fig. 5. Comparison of displacement time traces between the cylinder with an unattached endplate, ($g^* = 0.04$), and a cylinder with no endplate. The chosen normalized velocities, $(U^*/f^*)S$ correspond with the bull's eyes in Fig. 4. The intermittent switching between the upper and lower branch for the unattached endplate case is replaced by a much more periodic vibration when the endplate is removed.

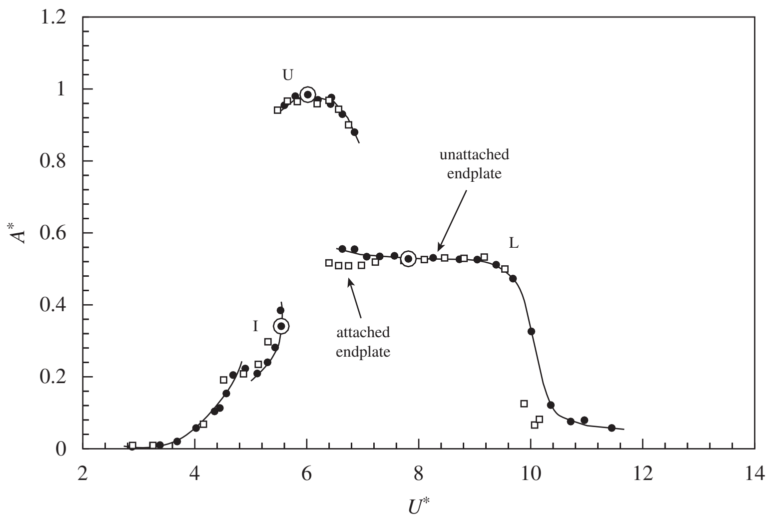

Fig. 6. Response amplitude (A^*) as a function of the normalized fluid velocity (U^*). Comparison between the unattached endplate case, ($g^* = 0.04$) (•), and attached endplate case (□). The responses are nearly identical for the two cases. Although not shown, the frequency data for the attached endplate case also agrees remarkably well with the unattached endplate case, shown in Fig. 3. The bull's eyes indicate the cases chosen to exhibit time traces of force in Figs. 7 and 8. $m^* = 9.3$, $(m^* + C_A)\zeta = 0.014$, Re = 5000−16 000.

4. Study of end conditions through controlled vibration

The whole investigation in this paper was actually stimulated by the wish to extensively measure fluid forces on a body that is controlled to vibrate in a sinusoidal transverse vibration, at extremely high resolution. This required very small increments of amplitude and frequency (Morse and Williamson, 2008). Obviously, with such an investment of effort to capture force contour plots, it was imperative to study very precisely the correct experimental conditions, from the outset. It was important to ensure we used the correct end boundary conditions for the oscillating cylinder. Our chosen experimental arrangement for the controlled vibrations is exactly the same as used for the free vibration experiments in Section 3, except the motion was controlled to be strictly sinusoidal. We conducted experiments to match the values of A^*, U^*/f^*, and Re from the free vibration response (case of an unattached endplate). These particular points in the initial, upper, and lower branches are shown by the bull's eye symbols in Fig. 6. For each chosen point, we run the controlled vibration either with an unattached endplate or without an endplate, and compare the measured forces.

In the initial branch, the fluid forcing is quite similar for both end conditions, as shown in Fig. 7. However, as expected, the forces start to exhibit some differences when one studies the upper branch; the maximum level of transverse force is approximately the same for each end condition, but there is more intermittency for the unattached endplate case. This is consistent with the free vibration experiments, where the upper branch is much steadier without an endplate. Nevertheless, prior to any experiments, one would have suspected the endplate would bring more periodicity.

In the lower branch, there are considerable differences between the two end conditions. For the case with an endplate in Fig. 8, the fluid force amplitude $C_Y(t)$ is quite steady. The phase angle, ϕ is just below 180°, yielding a small positive excitation per cycle ($C_Y \sin\phi$) if we were considering free vibration (see Eq. (4)). Without an endplate, the fluid forcing is much less steady, which would lead to the expectation that the response amplitude (if one had free vibration) would drop. However, we find that the phase angle has a mean value of 63°, even though it varies considerably, which would yield a much higher fluid excitation ($C_Y \sin\phi$). In essence, if the cylinder was freely oscillating at the amplitude used here ($A^* = 0.53$) and the endplate was removed, the energy into the system would then be much higher than the energy lost due to damping and the amplitude would increase. This is consistent with results from the free vibration experiments, where the absence of an endplate led to higher amplitudes.

In Section 1, for controlled vibrations using an unattached endplate, we showed from our early study that the fluid forces were significantly influenced by the gap between the bottom of the cylinder and the endplate (Fig. 1). Of course, one expects that with sufficient gap, the system would respond as though there were no endplate. We study now the effect of varying the endplate gap in the lower response branch, where the effect of end conditions is most pronounced. The variation in fluid excitation ($C_Y \sin\phi$) with gap ratio is shown in Fig. 9. For small gap ratios, where the gap is 10–15% of a diameter ($g^* = 0.1-0.15$), the excitation is roughly 0.1. However, for larger gaps, where g^* exceeds 15%, there is a large jump in the fluid excitation up to roughly 0.4, which corresponds well with the case without an endplate

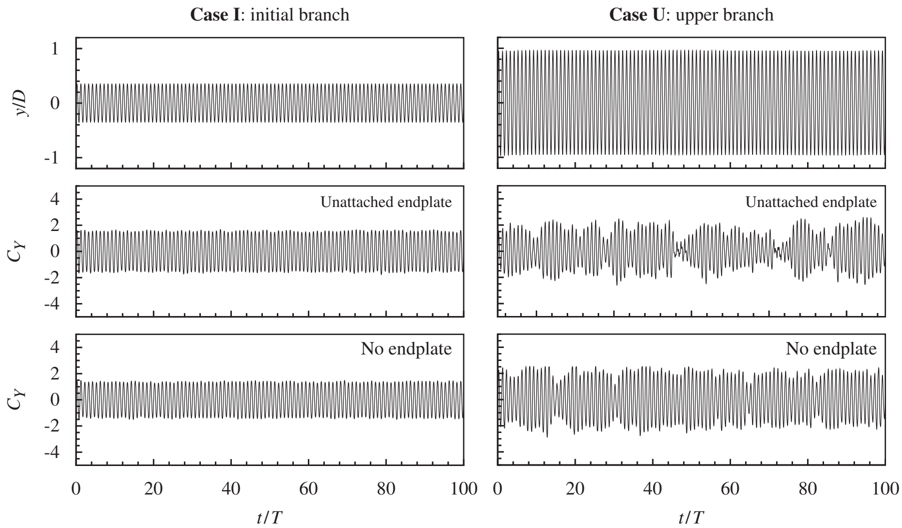

Fig. 7. Time traces of transverse force (C_Y) for an unattached endplate ($g^* = 0.04$), and for no endplate in the initial and upper branches of response. For both end conditions the motion of the cylinder (y/D) is controlled to be sinusoidal with $U^*/f^* = 6.0$, $A^* = 0.34$ in the initial branch, and with $U^*/f^* = 5.8$, $A^* = 0.98$ in the upper branch.

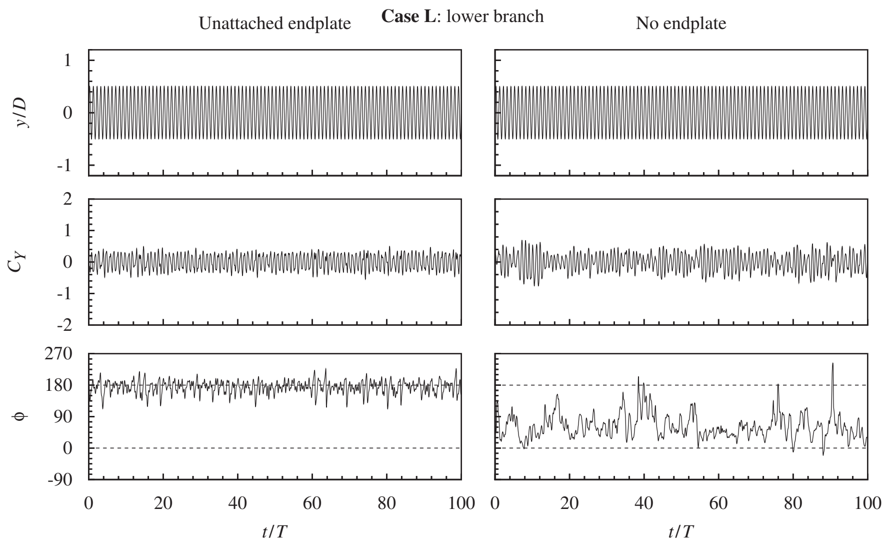

Fig. 8. Time traces of transverse force (C_Y) and phase angle (ϕ) for an unattached endplate ($g^* = 0.04$), and for no endplate. In both cases the motion of the cylinder (y/D) is controlled to be sinusoidal with $U^*/f^* = 7.2$ and $A^* = 0.53$, corresponding to the lower branch.

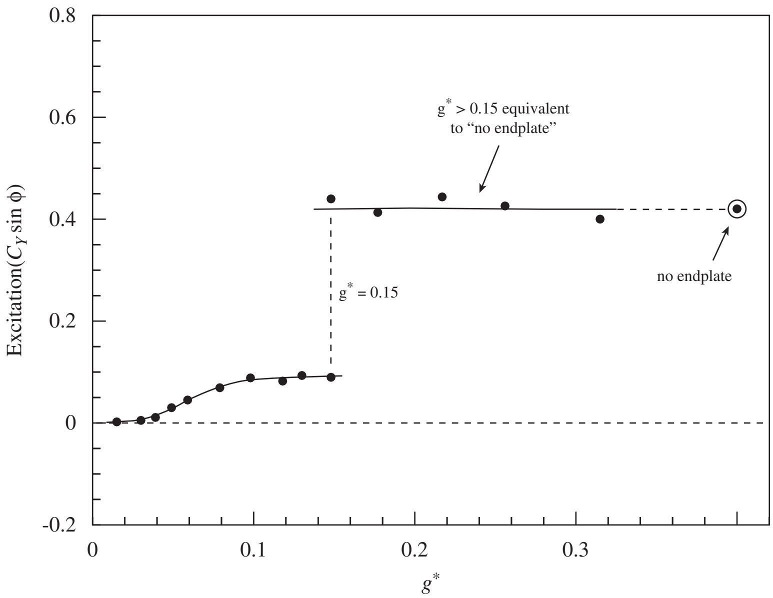

Fig. 9. The effect of endplate gap (g^*) on the fluid excitation ($C_Y \sin \phi$) for a cylinder with an unattached endplate. When the gap ratio is greater than 0.15, the fluid forcing is equivalent to the no endplate case. (At all points the motion of the cylinder is controlled to be sinusoidal with $U^*/f^* = 7.2$ and $A^* = 0.53$, corresponding to the lower branch.)

(included as the bull's eye in Fig. 9). This critical gap ratio ($g^* = 0.15$) is a useful result which suggests, for example, that with a 2.5 cm cylinder an endplate gap greater than 4 mm is the equivalent to having no endplate at all.

5. Comparison with previous investigations employing different end conditions

A summary of the characteristic low mass–damping free vibration responses for each of the end conditions in this study are presented for clarity in Fig. 10. One may compare the present results with free vibration responses taken from

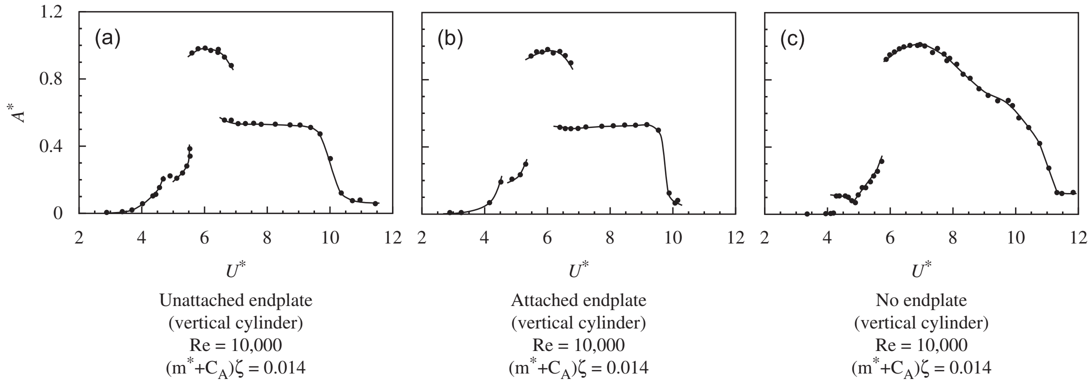

Fig. 10. A summary of the amplitude responses for each of the end conditions studied here: (a) unattached endplate, (b) attached endplate, (c) no endplate.

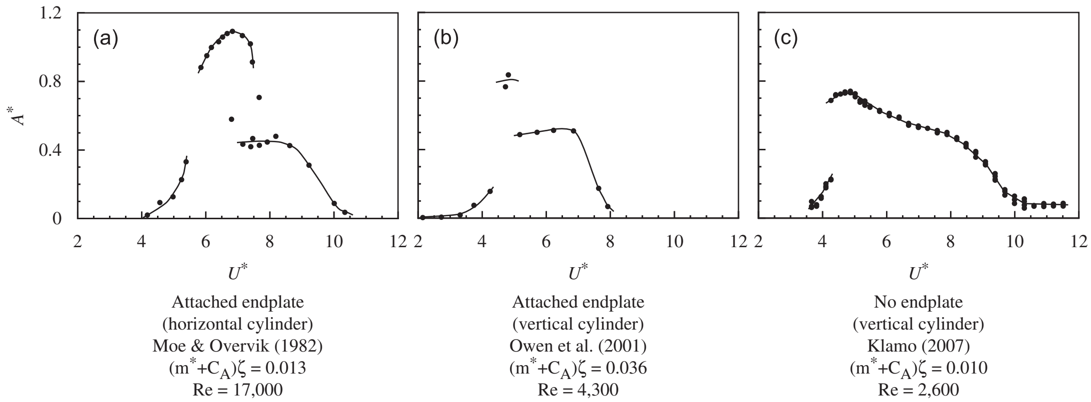

Fig. 11. Comparison among several previous vortex-induced vibration studies of the amplitude (A^*) response as a function of normalized velocity (U^*): (a) Moe and Overvik (1982), (b) Owen et al. (2001), and (c) Klamo (2007).

selected previous investigations, in Fig. 11. Cases where attached endplates are used (Moe and Overvik, 1982; Owen et al., 2001) exhibit good correspondence with our cases of unattached and attached endplates, showing three distinct response branches. On the other hand, Klamo (2007) did not use endplates in his experimental arrangement. His smallest gap with $g^* = 0.4$ should yield similar results to our case without an endplate, based on the results of our gap study (Fig. 9), and indeed the comparison of the character of the response plot is good. The response plot shows a gradual decrease in amplitude from the peak, rather than a distinct upper and lower branch. This type of response can be found in several other previous studies in the literature, and it remains possible that such responses are influenced by the end conditions, as shown in the present work.

In studies that did not employ endplates, the investigators generally took care in placing the bottom of the cylinder close to the channel floor (for example, Brankovic and Bearman, 2006). If the gap ratio is small enough ($g^* < 0.15$) we might expect that this end condition will yield a response that is similar to the case of an unattached endplate, as the two end conditions are quite similar. However, the experiment relies on the properties of the boundary layer on the channel floor which would depend on the channel construction (for example, the streamwise length of the boundary layer, or the existence of seams joining sections of the facility). Thus the boundary layer could be quite unsteady, and would certainly vary from one facility to the next, making comparisons difficult.

6. Conclusions

In this paper, we investigate the effect of end conditions on the transverse vortex-induced vibration response of a circular cylinder with low mass–damping. While we are able to vary the conditions at the lower end of a vertical cylinder in our water channel, all other aspects of the experimental arrangement are kept constant.

The case of an attached endplate and the case of an unattached endplate show nearly identical free vibration responses, although having an unattached endplate is simpler to arrange accurately, on a practical basis. However, the condition without an endplate shows significant differences. We expected, prior to this study, that removing an endplate would lead to increased fluid flow around the end of the cylinder, a reduction in spanwise vortex shedding correlation and fluid force correlation, and thereby to a reduced response amplitude. Quite contrary to this expectation, the absence of an endplate leads to significantly higher levels of excitation, leading to higher amplitudes over the entire amplitude response plot, except where both sets of data reach the same maximum amplitude. The increased excitation ($C_Y \sin\phi$) is principally due to a shift in the phase of the fluid force (relative to body motion). Essentially, the case without an endplate yields roughly the same peak amplitude response when compared to both cases with the endplates. The general character of the response is modified if the endplate is removed; the response amplitude diminishes continuously as velocity is increased beyond the value for peak amplitude, and there is no apparent jump between upper branch and lower branch modes.

Under conditions of controlled vibration, we also study the effect of varying the gap between an endplate and the bottom of the cylinder. For gaps larger than 15% of a diameter, we find a jump increase in the fluid excitation. Under these conditions, the force and response dynamics become equivalent to removing the endplate altogether. For smaller gaps, $g^* < 15\%$, one is effectively investigating the case of an attached or unattached endplate.

The character of response plots, in previous studies, correspond reasonably well with the character of the different responses found here, if one compares cases with similar end conditions. There are, of course, other aspects of the experimental arrangement besides end conditions, such as Reynolds numbers, turbulence levels, techniques of measurement, more degrees of freedom, and spanwise variations, that would lead to differences in the response character, but we suggest that end conditions should be taken into account as influencing quite significantly the character of a response plot. It is, however, interesting that the peak amplitude response is not strongly influenced by the end conditions, at least based on the present results.

Acknowledgements

The support from the Ocean Engineering Division of ONR, monitored by Dr Tom Swean, is gratefully acknowledged (ONR Contract Nos. N00014-04-1-0031 and N00014-07-1-0303). The authors would also like to thank Matthew Horowitz for his enthusiastic and helpful input to this research.

References

Anand, N.M., Tørum, A., 1985. Free span vibration of submerged pipelines in steady flow and waves. In: Proceedings of the International Symposium on Separated Flow Around Marine Structure, Trondheim, Norway, pp. 155–199.

Bearman, P.W., 1984. Vortex shedding from oscillating bluff bodies. Annual Review of Fluid Mechanics 16, 195–222.

Brankovic, M., Bearman, P.W., 2006. Measurements of transverse forces on circular cylinders undergoing vortex-induced vibration. Journal of Fluids and Structures 22, 829–836.

Govardhan, R., Williamson, C.H.K., 2000. Modes of vortex formation and frequency response of a freely vibrating cylinder. Journal of Fluid Mechanics 420, 85–130.

Govardhan, R.N., Williamson, C.H.K., 2005. Revealing the effect of Reynolds number on vortex-induced vibrations using controlled negative and positive damping. In: Proceedings of the 4th Conference on Bluff Body Wakes and Vortex-Induced Vibration (BBVIV-4), Santorini, Greece.

Govardhan, R.N., Williamson, C.H.K., 2006. Defining the 'modified Griffin plot' in vortex-induced vibration: revealing the effect of Reynolds number using controlled damping. Journal of Fluid Mechanics 561, 147–180.

Griffin, O.M., Ramberg, S.E., 1982. Some recent studies of vortex shedding with application to marine tubulars and risers. ASME Journal of Energy Resource Technology 104, 2–13.

Hover, F.S., Techet, A.H., Triantafyllou, M.S., 1998. Forces on oscillating uniform and tapered cylinders in crossflow. Journal of Fluid Mechanics 363, 97–114.

Hover, F.S., Davis, J.T., Triantafyllou, M.S., 2004. Three-dimensionality of mode transition in vortex-induced vibrations of a circular cylinder. European Journal of Mechanics B—Fluids 23, 29–40.

Jauvtis, N., Williamson, C.H.K., 2004. The effect of two degrees of freedom on vortex-induced vibration at low mass and damping. Journal of Fluid Mechanics 509, 23–62.

Khalak, A., Williamson, C.H.K., 1996. Dynamics of a hydroelastic cylinder with very low mass and damping. Journal of Fluids and Structures 10, 455–472.

Khalak, A., Williamson, C.H.K., 1999. Motions, forces and mode transitions in vortex-induced vibrations at low mass-damping. Journal of Fluids and Structures 13, 813–851.

Klamo, J.T., 2007. Effects of damping and Reynolds number on vortex-induced vibrations. Ph.D. Thesis, Caltech.

Klamo, J.T., Leonard, A., Roshko, A., 2005. On the maximum amplitude for a freely vibrating cylinder in cross-flow. Journal of Fluids and Structures 21, 429–434.

Klamo, J.T., Leonard, A., Roshko, A., 2006. The effects of damping on the amplitude and frequency response of a freely vibrating cylinder in cross-flow. Journal of Fluids and Structures 22, 845–856.

Moe, G., Overvik, T., 1982. Current-induced motions of multiple risers. In: Chryssostomides, C., Connor, J.J. (Eds.), Proceedings of BOSS-82, Behaviour of Offshore Structures. Hemisphere, Washington, DC, pp. 618–639.

Morse, T.L., Williamson, C.H.K., 2006. Employing controlled vibrations to predict fluid forces on a cylinder undergoing vortex-induced vibration. Journal of Fluids and Structures 22, 877–884.

Morse, T.L., Williamson, C.H.K., 2008. Prediction of response branches, wake modes, and transitions in vortex-induced vibration through controlled motion. Journal of Fluid Mechanics; submitted.

Owen, J.C., Bearman, P.W., Szewczyk, A.A., 2001. Passive control of VIV with drag reduction. Journal of Fluids and Structures 15, 597–605.

Parkinson, G., 1989. Phenomena and modelling of flow-induced vibrations of bluff bodies. Progress in Aerospace Sciences 26, 169–224.

Prasad, A., Williamson, C.H.K., 1997. Three dimensional effects in turbulent bluff-body wakes. Journal of Fluid Mechanics 343, 235–264.

Sarpkaya, T., 1979. Vortex-induced oscillations. Journal of Applied Mechanics 46, 241–258.

Sarpkaya, T., 1995. Hydrodynamic damping, flow-induced oscillations, and biharmonic response. ASME Journal of Offshore Mechanics and Arctic Engineering 117, 232–238.

Slaouti, A., Gerrard, J.H., 1981. An experimental investigation of the end effects on the wake of a circular-cylinder towed through water at low Reynolds numbers. Journal of Fluid Mechanics 122, 297–314.

Stansby, P.K., 1974. Effects of end plates on base pressure coefficient of a circular cylinder. Aeronautical Journal 78, 36–37.

Szepessy, S., Bearman, P.W., 1992. Aspect ratio and end plate effects on vortex shedding from a circular cylinder. Journal of Fluid Mechanics 234, 191–217.

Vikestad, K., Vandiver, J.K., Larsen, C.M., 2000. Added mass and oscillation frequency for a circular cylinder subjected to vortex-induced vibrations and external disturbance. Journal of Fluids and Structures 14, 1071–1088.

Williamson, C.H.K., 1988. Defining a universal and continuous Strouhal–Reynolds number relationship for the laminar vortex shedding of a circular cylinder. Physics of Fluids 31, 2742–2744.

Williamson, C.H.K., 1989. Oblique and parallel modes of vortex shedding in the wake of a circular cylinder at low Reynolds numbers. Journal of Fluid Mechanics 206, 579–627.

Williamson, C.H.K., 1996. Vortex dynamics in the wake. Annual Review of Fluid Mechanics 28, 477–539.

Williamson, C.H.K., Govardhan, R., 2004. Vortex-induced vibrations. Annual Review of Fluid Mechanics 36, 413–455.